

TRACKING PERFORMANCE IMPROVEMENT OF A MAGNETIC LEVITATION STAGE USING TWO DEGREES-OF-FREEDOM H_∞ LOOP SHAPING CONTROLLER

Oui-Serg Kim

Institute of Advanced Machinery and Design at Seoul National Univ., Korea, oskim@amed.snu.ac.kr

Dong-Chul Han

School of Aerospace and Mechanical Eng., Seoul National Univ. Seoul, Korea, dchan@amed.snu.ac.kr

In-Bae Chang

Dept. of Mechatronics Eng., Kangwon National Univ., Chuncheon, Korea, inbae@cc.kangwon.ac.kr

Sang-Ho Lee

Institute of Advanced Machinery and Design at Seoul National Univ., Korea, leesang@amed.snu.ac.kr

ABSTRACT

This paper presents a **tracking performance** improvement of a **magnetic levitation stage** supported by linear magnetic bearings using two degrees-of-freedom(TDF) controller. The most important part in the design of a TDF H_∞ loop shaping controller is to select a proper weighting function and reference model. We present a design guide derived from the evaluation of the performance in experiment, which is obtained by modifying the parameter in the weighting function and reference model.

1. INTRODUCTION

A magnetic bearing using an attractive magnetic force is inherently unstable and the control objective includes feedback stabilization. McFarlane and Glover proposed a systematic H_∞ loop-shaping design procedure[1][2]. The procedure has a structure of a single degree-of-freedom(SDF) control using a feedback signal only as an input to the controller. It provides a robust stabilization and can specify a robust performance specification in frequency domain. However, in cases where stringent time domain specifications are set on the output response, a SDF structure is not sufficient. To use the magnetic levitation(maglev) stage as a precision positioning device, it requires not only stable levitation and robust disturbance rejection in the frequency domain but also essentially needs several dynamic characteristics such as faster settling time and less overshoot in the time domain. These requirements can be met with the TDF controller that is designed to fulfill the specifications in the frequency domain and also in the time domain.

In this paper, we describe the **two degrees-of-freedom(TDF) control** design procedure to apply to the magnetic levitation stage and demonstrate the enhanced tracking performance from the experiment

results in the step response.

This paper is laid out as follows. Section 2 summarizes basic results relating to the H_∞ loop shaping method of McFarlane-Glover and to its TDF extension based on Hoyle and Limebeer. In section 3, the model of the maglev stage is described in state-space form. Performance evaluation and the main result of this paper will be presented in section 4. Finally we conclude this paper in section 5.

2. H_∞ LOOP SHAPING DESIGN

2.1 SDF Loop Shaping Controller

This section is to summarize the approach of loop shaping procedure based on H_∞ robust stabilization combined with classical loop shaping. This approach makes use of an uncertainty description based on an additive perturbations to a normalized coprime factorization of the plant. A normalized left coprime factorization of a plant G is given by $G = M^{-1}N$ where M and N are coprime matrices in RH_∞ . Robustness with respect to additive perturbations to the normalized coprime factors is considered. A perturbed plant model G_p can be written as

$$G_p = (M + \Delta_M)^{-1}(N + \Delta_N) \quad (1)$$

The objective of robust stabilization is to stabilize both nominal G and perturbed plant G_p defined by eq(2).

$$G_\varepsilon = \{ G_p : [\Delta_M, \Delta_N] \in RH_\infty^{p \times (p+m)}, \|\Delta_M, \Delta_N\|_\infty < \varepsilon \} \quad (2)$$

where ε is the stability margin.

To maximize this stability margin is the problem of robust stabilization of normalized coprime factor plant description. For the perturbed feedback system of FIGURE 1, the stability property is robust iff the nominal feedback system is stable and a target norm bound γ for H_∞ optimization is given by eq(3).

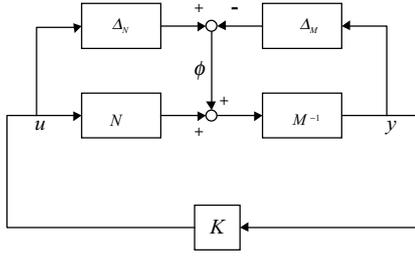


FIGURE 1: Schematic of H_∞ Robust Stabilization Problem

$$\varepsilon_{\max}^{-1} = \gamma_{\min} = \inf_K \left\| \begin{bmatrix} K \\ I \end{bmatrix} (I - GK)^{-1} \tilde{M}^{-1} \right\|_\infty \quad (3)$$

A controller which guarantees eq(4) is given by eq(5).

$$\left\| \begin{bmatrix} K \\ I \end{bmatrix} (I - GK)^{-1} \tilde{M}^{-1} \right\|_\infty \leq \gamma \quad (4)$$

where

$$K = \left[\begin{array}{c|c} A + BF + \gamma^2(L^T)^{-1}ZC^T(C + DF) & \gamma^2(L^T)^{-1}ZC^T \\ \hline B^T X & -D^T \end{array} \right] \quad (5)$$

$$F = -S^{-1}(D^T C + B^T X) \quad (5)$$

$$L = (1 - \gamma^2)I + XZ.$$

The basic stages in the procedure consist of open loop augmentation of the nominal plant by pre- and post-weighting functions, W_1 and W_2 respectively. This frequency dependent weighting functions are chosen to improve the open loop system's singular value frequency response and specify the performance in frequency domain. The shaped plant G_s and the controller is given by eq(6)

$$G_s = W_2 G W_1, K = W_1 K_s W_2 \quad (6)$$

2.2 TDF Loop Shaping Controller

The configuration to use for the TDF design is shown in FIGURE 2. In Hoyle[3] and Limebeer[4], a TDF extension of the McFarlane-Glover procedure was proposed to enhance the model-matching properties of the closed-loop and Walker[5] reported on the structure of a TDF controller. The proposed controller is composed by a feedback and a feedforward part. The feedback controller is applied to provide robust stabilization, while the feedforward controller is introduced to force the response of the closed-loop system to follow that of the reference model M_o . M_o is the desired closed-loop transfer function selected by the designer to introduce time-domain specifications.

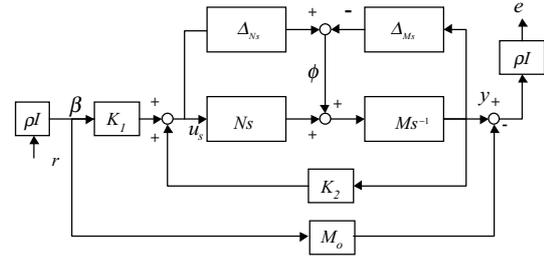


FIGURE 2: TDF H_∞ loop shaping design problem

The design problem is to find the stabilizing controller K for the shaped plant $G_s = G W_1$.

The control signal u_s to the shaped plant is given by

$$u_s = [K_1 \quad K_2] [\beta \quad y]^T \quad (7)$$

Where K_1 is the prefilter, K_2 is the feedback controller, β is the scaled reference, ρ is a scalar parameter that the designer can increase to place more emphasis on model matching and y is the measured output. The purpose of the prefilter is to ensure eq(8).

$$\left\| (I - G_s K_2)^{-1} G_s K_1 - M_o \right\|_\infty \leq \gamma \rho^{-2} \quad (8)$$

To put the TDF design problem into the standard control configuration, a generalized plant P is defined by eq(9).

$$\begin{bmatrix} u_s \\ y \\ e \\ \beta \\ y \end{bmatrix} = \begin{bmatrix} P_{11} & P_{12} \\ P_{21} & P_{22} \end{bmatrix} \begin{bmatrix} r \\ \phi \\ u_s \end{bmatrix} = \begin{bmatrix} 0 & 0 & I \\ 0 & M_s^{-1} & G_s \\ \rho^2 M_o & M_s^{-1} & \rho G_s \\ \rho I & 0 & 0 \\ 0 & M_s^{-1} & G_s \end{bmatrix} \begin{bmatrix} r \\ \phi \\ u_s \end{bmatrix} \quad (9)$$

Putting

$$M_o s = \begin{bmatrix} A_o & B_o \\ C_o & D_o \end{bmatrix}, G_s s = \begin{bmatrix} A_s & B_s \\ C_s & D_s \end{bmatrix} \quad (10)$$

with M_o chosen stable, and substituting into eq(9) gives P .

$$\begin{bmatrix} A_s & 0 & 0 & (B_s D_s^T + Z_s C_s^T) R_s^{-1/2} & B_s \\ 0 & A_o & B_r & 0 & 0 \\ 0 & 0 & 0 & 0 & I \\ C_s & 0 & 0 & R_s^{1/2} & D_s \\ C_s & -\rho^2 C_o & -\rho^2 D_r & \rho R_s^{1/2} & \rho D_s \\ 0 & 0 & \rho I & 0 & 0 \\ C_s & 0 & 0 & R_s^{1/2} & D_s \end{bmatrix} \quad (11)$$

The controller K satisfying eq(12) could be computed using a standard software package like "MATLAB"

$$\|F(P, K)\|_\infty < \gamma \quad (12)$$

The command signals r can be scaled by a constant matrix W_i to make the closed-loop transfer function from r to the controlled outputs y match the desired model M_o exactly at steady-state. The required scaling is given by eq(13)

$$W_i \triangleq \left[(I - G_s(0)K_2(0))^{-1} G_s(0)K_1(0) \right]^{-1} M_o(0) \quad (13)$$

Thus, the resulting controller is $K=[K_1W_i \ K_2]$. Skogestad et al[7] summarized the main steps required to synthesize a TDF H_∞ loop-shaping controller and showed the final TDF H_∞ loop-shaping controller as illustrated in FIGURE 3.

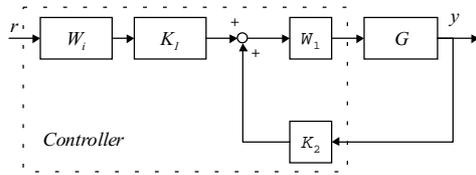


FIGURE 3: TDF H_∞ loop shaping controller

3. PLANT MODELLING

3.1 Maglev Stage

FIGURE 4 shows the schematic of the maglev system composed of six guideways, four bearing modules, a maglev stage, a linear motor, a linear scale and a sensor amplifier.

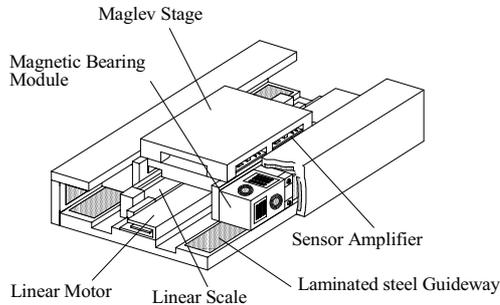


FIGURE 4: Schematic of the Maglev System

Four magnetic bearing modules are attached to the maglev stage. Each of the magnetic bearing modules consists of three electromagnetic actuators and three capacitive sensors. The capacitive sensor system is used as a displacement feedback device. Both the actuator and the sensor are laid on the same surface of the module and are molded with epoxy. The guideways are made of laminated silicon steel to reduce energy loss due to the eddy current.

3.2 Equation of Motion

From this section, the equation of motion yields a state-space equation. The equation of motion for the stage as shown in FIGURE 5 is given by

$$\begin{aligned} m\ddot{z} &= \sum f_z - mg = f_1 + f_2 + f_3 + f_4 - mg \\ m\ddot{y} &= \sum f_y = f_5 + f_6 \end{aligned} \quad (14)$$

$$J\ddot{\varphi}_{x,y,z} = \sum_{j=1}^6 r_j \times f_j$$

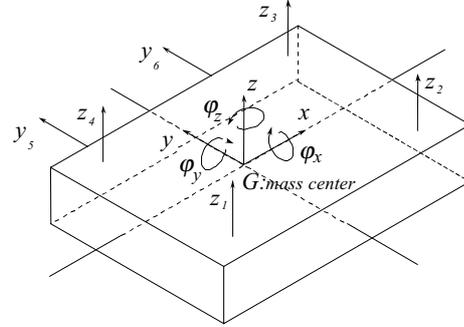


FIGURE 5: Convention Coordinate of the Maglev System

where r_j represents the displacement vector from the mass center of the maglev stage to the geometric center of the j^{th} channel of the magnetic bearing module and f_y, f_z is the external force of the magnetic bearing in the y, z directions respectively.

The maglev system yields an equation for five-degree-of-freedom in the form

$$M\ddot{q} = N_A F - mg \quad (15)$$

where F is the resultant force of the magnetic bearing. Each of the modules is located almost symmetrically, so the mass-inertia matrix M can be assumed to be diagonal. q is a base coordinate for translation and angular motion, and N_A is a linear transformation matrix from q to the actuator coordinates:

$$M = \begin{bmatrix} m & & & & \\ & m & & & \\ & & J_x & & \\ & & & J_y & \\ & & & & J_z \end{bmatrix}$$

$$q = [y \quad z \quad \varphi_x \quad \varphi_y \quad \varphi_z]^T \quad (15)$$

3.3 Magnetic Bearing Force

Each magnetic bearing channel consists of a pair of opposite electromagnets, and it has a resultant magnetic force f_j given by equation (17) which is combined of a displacement-force with position stiffness k_{sj} and a current-force with current stiffness k_{ij} .

$$f_j = k_{sj}x_j + k_{ij}i_j \quad (17)$$

$$k_{xj} = \frac{\mu_0 A n^2 i_{bj}^2}{2g_0^3}, k_{yj} = \frac{\mu_0 A n^2 i_{bj}^2}{2g_0^2}$$

where permeability of air μ_0 is $4\pi \times 10^{-7}$, nominal air gap g_0 is 0.3 mm and pole face area A of each magnetic bearing is $266.2 \times 10^{-6} m^2$, and coil turns n are 330. The total magnetic force acting on the maglev stage can be expressed as

$$F = K_X N_A q + K_1 i \quad (18)$$

where

$$K_X = \text{diag}[k_{xz} \quad k_{xz} \quad k_{xz} \quad k_{xz} \quad k_{xy} \quad k_{xy}]$$

$$i = [i_1 \quad i_2 \quad i_3 \quad i_4 \quad i_5 \quad i_6]^T$$

$$K_1 = \text{diag}[k_{iz} \quad k_{iz} \quad k_{iz} \quad k_{iz} \quad k_{iy} \quad k_{iy}]$$

Substituting equation (18) into equation (15) yields

$$\ddot{q} = M^{-1} N_A^T K_X N_A q + M^{-1} N_A^T K_1 i + N_g g \quad (19)$$

where

$$N_g = [0 \quad -1 \quad 0 \quad 0 \quad 0]^T$$

3.4 State-Space Representation

Although the maglev stage has six degrees of freedom, only five coordinates ($y, z, \varphi_x, \varphi_y, \varphi_z$) are required to control five degrees of freedom at the target position moved by the linear motor. There are six sensor channels in the fabricated system for symmetry, but five channels are only needed to measure the five-degree-of-freedom motions. Thus we use two channels for y and φ_z motions in the y plane and three channels for z, φ_x and φ_y motions in the z plane. Therefore, the whole system can be described as a five-input/six-output system. The state-space representation obtained from the equation of motion can be described as follows:

$$\dot{X} = A X + B U + B_g g \quad (20)$$

$$Y = C X + D U$$

where

$$A = \left[\begin{array}{c|c} O_{5 \times 5} & I_{5 \times 5} \\ \hline N_S M^{-1} N_A^T K_X N_A N_S^{-1} & O_{5 \times 5} \end{array} \right]$$

$$B = \left[\begin{array}{c} O_{5 \times 6} \\ \hline N_S M^{-1} N_A^T K_1 K_{amp} \end{array} \right], B_g = \left[\begin{array}{c} O_{5 \times 1} \\ \hline N_S M^{-1} N_g \end{array} \right]$$

$$C = [K_S \mid O_{5 \times 5}], D = [O_{5 \times 6}]$$

The output of the system representing the displacement of each magnetic bearing has a unit of voltage, thus the sensor gain K_S should be multiplied by the real output Y to convert from a unit of metre.

4. SIMULATION AND EXPERIMENTAL RESULTS

As described in section 2, we synthesize a SDF and a TDF controller to control the maglev stage. Each controller has 16 and 26 states so that the controllers are reduced for digital implementation to the same states of 10. To minimize degradation of a step response due to the controller reduction [7], we use a balanced residualization method.

4.1 Selection of the Weighting Function for SDF Controller

Following the prescriptive procedure given in section 2, the loop shaping weighting function was selected. We can specify the required dynamic characteristics for the plant and the relative importance of the controlled output from the singular value plot of the open loop system via W_1, W_2 respectively.

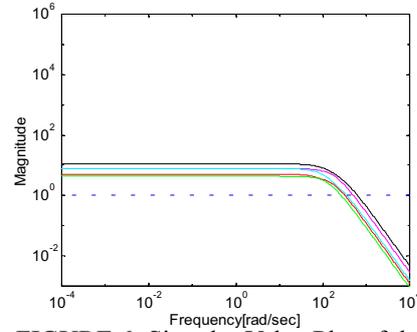


FIGURE 6: Singular Value Plot of the Plant

FIGURE 6 shows the singular values of the plant and the plant need extra low frequency gain to give good steady-state tracking and disturbance rejection. W_2 was chosen as a constant identity matrix because all of the sensor outputs indicating the position of the actuator have the same importance. W_1 we decided on was

$$W_1 = 2 \frac{s+20}{s+0.001} \quad (21)$$

i.e. Integrator boosts low frequency gain but the integrator without pole and zero yields a low bandwidth of 10 rad/sec. Therefore, we introduced the phase-advance term $s+20$ to increase the bandwidth and reduce the roll-off rate close to -1 at cross-over frequency. The pole makes the integral action start from 0.001rad/sec. We multiply the gain by a factor 2 to make the response a little faster. FIGURE 7 shows the singular values of the shaped plant.

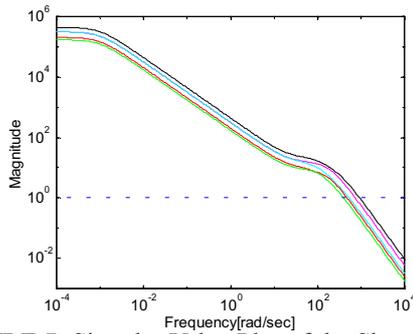


FIGURE 7: Singular Value Plot of the Shaped Plant

Finally we synthesized 16 states controller and reduced to 10 states. FIGURE 8,9 shows the step response in z-axis of the maglev stage with the full-order SDF controller and reduced controller respectively.

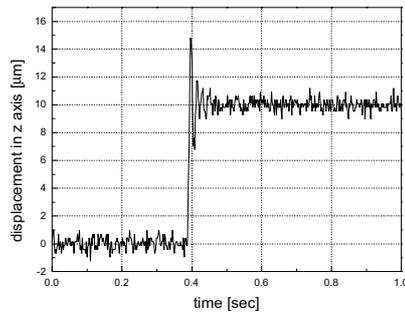


FIGURE 8: Step Response of the Full-order SDF

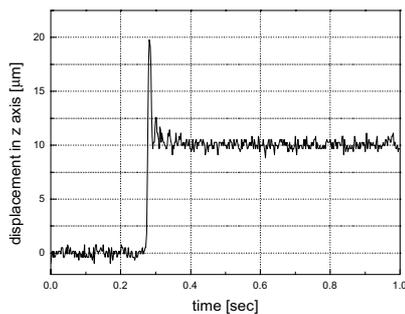


FIGURE 9: Step Response of the Reduced SDF

Full-order controller exhibits rising time less than 20ms and settling time of 100ms but is oscillatory. It needs more damping. The reduced controller shows large overshoot. In case of SDF controller, the parameter cannot be modified widely because it doesn't have an extra damping adjustment so that it cannot compensate the stiff roll-off rate near the cross-over frequency. To improve the tracking performance, the TDF controller will be considered in the next subsection.

4.2 Selection of the Weighting Function for TDF Controller

The same weighting function was chosen for W_1 in the TDF controller to evaluate a performance of the TDF controller. The reference step response model was selected to be second-order mass-damper-spring system and is given by

$$M_o = \frac{\omega_n^2}{s^2 + 2\zeta\omega_n s + \omega_n^2} \quad (22)$$

The undesirable overshoot and oscillatory step response of the SDF controlled plant can be compensated by the damping factor ζ . The second order system gives a maximum overshoot OS to a unit step demand

$$OS = \exp(-\pi\zeta / (1 - \zeta^2)^{1/2}) \quad (23)$$

So we need a damping factor ζ for a given overshoot OS .

$$\zeta = \frac{-\ln OS}{(\pi^2 + (\ln OS)^2)^{1/2}} \quad (24)$$

The last parameter ω_n was selected near by the bandwidth shown in singular value plot of the shaped plant.

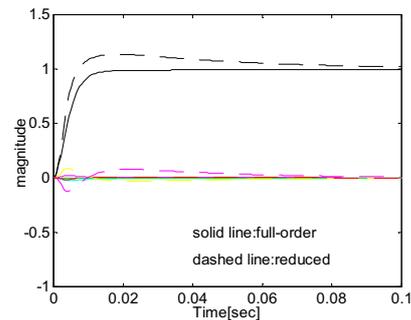


FIGURE 10: Step Response of the TDF controlled Plant in Simulation

FIGURE 10 shows the step response of the full-order and reduced TDF controller in simulation. The reduced controller shows faster rising time but it has longer settling time than full-order controller. Therefore, we changed the whole parameters in the weighting function and reference model to evaluate the performance. TABLE 1 summarizes the experimental results. The experimental result present that damping factor ζ , gain and zero of weighting function W_1 have a large effect on the settling time property. The overshoot is affected by ζ and ω_n . Especially for small value of ω_n , the plant had very large overshoot, which is not undesirable.

TABLE1: Design Guidance for TDF Loop Shaping

	Overshoot	Rising time	Settling time	Range
OS(ζ)	○	▲	⊙	0.1 → 0.0001
Gain	▲	▲	⊙	1.2 → 3
Pole	▲	×	○	-0.1 → -0.0001
Zero	○	×	⊙	-10 → -100
ω_n	⊙	×	▲	100 → 1000

○: have effect, ▲: small effect, ⊙:large effect, ×:none.

Some properties in the table are not agree with the theoretical result in the literature exactly but this table helps intuitive selection for the parameter modification. Following this table, the final controller has a weighting function and a reference model given in eq(25) and eq(26).

$$W_1 = 2 \frac{s + 100}{s + 0.0001} \tag{25}$$

$$M_o = \frac{2500}{s^2 + 2(0.9647)(500)s + 2500} \tag{26}$$

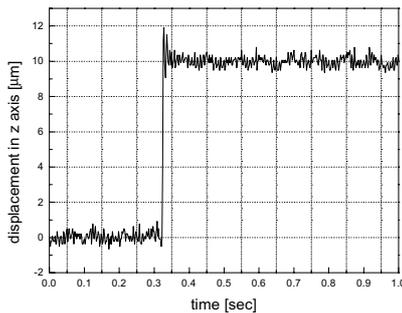


FIGURE 11: 10 µm Step Response in z-axis of the Enhanced Plant

FIGURE 11 shows the 10 µm step response of the plant using final TDF controller and has 2 µm overshoot, 25ms settling time. Therefore, the time response turns out to be improved and the TDF controller is recommended for positioning system.

5. CONCLUSION

The TDF H_∞ controller was used to improve the tracking performance of magnetically levitated stage. We have addressed time response specifications to the SDF H_∞ loop shaping control by introducing a reference step response model. The TDF controller that can address the time response specification has high order states. To reduce the states of controller for practical implementation, we have adopted a balanced residualization to minimize the performance deterioration but realized that the step response was still

delayed by the reduction. We evaluated the performance of the step response according to the parameter modification in the weighting function and the reference model. Through this study, we presented that the TDF H_∞ loop shaping controller is suitable for tracking performance improvement and can be designed by more intuitive way that allows to predict the step response.

ACKNOWLEDGEMENTS

This research is based upon National Research Projects supported by the Institute of Advanced Machinery & Design and Turbo & Power Machinery Research Center at Seoul National University and Samsung Electronics.

REFERENCES

- McFarlane D. and Glover K., A Loop Shaping Design Procedure Using H_∞ Synthesis, IEEE Transactions on Automatic Control AC-37(6), pp. 759-769, 1992.
- McFarlane D. and Glover K., Robust Controller Design Using Normalized Coprime Factor Plant Descriptions, Lecture Notes in Control and Information Sciences, Springer-Verlag, 1990
- Hoyle D., Hyde R. and Limebeer D., An H_∞ approach to two degree of freedom design, Proc. of the 30th IEEE Conf. On Decision and Control, 1991, pp. 1581-1585.
- Limebeer D., Kasenally E. and Perkins J., On the design of robust two degree of freedom controllers, Automatica, 29, 1993, pp. 157-168.
- Walker D.J., On the Structure of a Two-Degree-of-Freedom H_∞ Loop Shaping Controller, Int. Journal of Control, vol. 63, No. 6, 1996, pp. 1105-1127.
- Hyde, R.A., The Application of Robust Control to VSTOL Aircraft, Ph.D thesis, University of Cambridge, 1991
- Skogestad S. and Postlethwaite I., Multivariable Feedback Control : Analysis and Design, John Wiley & Sons, 1996.